Proceedings of the 1st international Symposium on AI and Fluid Mechanics
Paper No S16 P3

Koopman-Inspired Operator Learning for Intrinsic Flame Instabilities

Rixin Yu [1] and Erdzan Hodzic[2]

[1]Department of Energy Sciences, Lund University, 22100 Lund, Sweden
[2]Department of Manufacturing Processes, Research Institutes of Sweden, 553 22 Jonkoping, Sweden

Abstract. We introduce the Koopman-inspired Fourier Neural Operator (kFNO) for predicting complex flame instabilities governed by nonlinear PDEs. Leveraging Koopman theory to lift dynamics into a high-dimensional latent space, kFNO improves short-term accuracy and long-term statistical fidelity. We validate kFNO on synthesized flame fronts from re-scaled Sivashinsky equations (modeling hybrid Darrieus-Landau and Diffusive-Thermal instabilities) and on large-scale DNS data of DL-unstable flames. Compared to the baseline FNO, kFNO achieves 2–6 times lower errors, more accurate dispersion relations, and superior computational efficiency, demonstrating its promise for efficient operator learning in chaotic, high-dimensional systems.

1. Introduction

Partial differential equations (PDEs) govern many physical phenomena—from fluid dynamics and climate modeling to combustion and plasma physics—but solving nonlinear, chaotic PDEs is computationally expensive due to the high-resolution discretization required by traditional methods (finite difference, finite element, spectral, etc.). Recently, operator learning via machine learning (ML) has emerged as an efficient alternative by learning mappings between function spaces, as demonstrated by DeepONet [1], Fourier Neural Operators (FNO) [2].However, these methods often struggle to maintain long-term accuracy in chaotic regimes where errors can rapidly amplify.

A key challenge is accurately learning the time-advancement operator that predicts future states from past data—a necessity in turbulence modeling, weather forecasting, and combustion simulations. Koopman operator theory [3, 4, 5] offers a robust framework by lifting nonlinear dynamics into a higher-dimensional latent space where evolution is approximately linear. Motivated by this, we introduced the Koopman-inspired Fourier Neural Operator (kFNO) [6], which leverages a high-dimensional representation to enhance both short-term accuracy and long-term statistical fidelity while remaining computationally efficient.

In this work, we extend our previous evaluation of kFNO in two ways. First, we apply kFNO to flame front data driven by hybrid Darrieus-Landau (DL) and Diffusive-Thermal (DT) instabilities [7, 8, 9], more representative of realistic combustion. Second, we test its robustness on large-scale DNS data of reactive flows exhibiting complex, fractal-like flame structures with unburned fuel pockets [10], providing a stringent benchmark for operator learning in highly nonlinear, noisy settings.

2. Problem Setup and Operator Learning Method

We aim to learn an n-step solution advancement operator for a time-dependent PDE:

$$\bar{G}_n : V \to V^n, \quad \phi(x,t) \mapsto (\phi(x,t_1), \ldots, \phi(x,t_n)), \tag{1}$$

where $t_j = t + j\Delta_t$, $V(\mathscr{D}, \mathbb{R}^{d_v})$ denotes functions on a d-dimensional spatial domain $\mathscr{D} \subset \mathbb{R}^d$, and V^n is the n-fold Cartesian product of V. In this framework, the multi-step operator $\bar{G}_n$ relates to the single-step operator $G \equiv \bar{G}_1$ via $\bar{G}_n = (G^1, \ldots, G^n)$, with G^m denoting m repeated applications of G. We approximate $\bar{G}_n$ with a neural network $\bar{\mathscr{G}}_n : V \times \Theta \to V^n$, where Θ is the set of trainable parameters. Prior work [11, 12, 13] focused on learning G using a network $\mathscr{G} \equiv \bar{\mathscr{G}}_1$, whose recurrent application enables long-horizon predictions. To improve stability, training is performed in a one-to-many fashion

with data $\{v_j,(G^1v_j,\ldots,G^nv_j)\}_{j=1}^Z$, by minimizing $\min_{\theta\in\Theta}\mathbb{E}\Big[C\big((\mathscr{G}^1v,\ldots,\mathscr{G}^nv),\bar{G}_nv\big)\Big]$, where $C(a,b)=\|a-b\|_2/\|b\|_2$ denotes the relative L2 error. In [6], we proposed directly learning $\bar{G}_n$ via $\min_{\theta\in\Theta}\mathbb{E}\Big[C\big(\bar{\mathscr{G}}_nv,\bar{G}_nv\big)\Big]$, allowing arbitrarily long predictions by iterative updates using the last output. The Koopman-inspired Fourier Neural Operator (kFNO) extends FNO by representing

$$\bar{\mathscr{G}}_n=\bar{P}\circ\bar{Q}\circ\bar{K}\circ H\circ L. \tag{2}$$

Here, the lifting map $L:V\to V_*$, implemented via an Multilayer perceptron(MLP), elevates $\phi(x,t)$ to a higher-dimensional space $V_*(\mathbb{R}^d;\mathbb{R}^{d_\varepsilon})$ with $d_\varepsilon>d_v$. A hidden map $H:V_*\to V_*$ refines this representation before the Koopman-like map $\bar{K}:V_*\to V_*^n$ advances the state via $\varepsilon_j(x)=A^j\varepsilon_0(x)$, with $A:V_*\to V_*$ approximating the Koopman operator. A further hidden map $Q:V_*\to V_*$ is applied elementwise through $\bar{Q}:V_*^n\to V_*^n$, and the projection $\bar{P}$ (an MLP $P:V_*\to V$) maps the result back to the solution space.
Maps H, A, and Q are constructed by stacking modified Fourier layers $F_s:V_*\to V_*$:

$$F_s(\varepsilon)=\sigma\Big(\mathscr{C}_{\not s}\Big(W\varepsilon+b+\mathscr{F}_s^{-1}\big\{\mathscr{R}(\mathscr{F}_s\{\varepsilon\})\big\}\Big)\Big), \tag{3}$$

with trainable $W\in\mathbb{R}^{d_\varepsilon\times d_\varepsilon}$, $b\in\mathbb{R}^{d_\varepsilon}$, activation σ, Fourier transforms $\mathscr{F}_s$ and $\mathscr{F}_s^{-1}$ over dimensions $s\subseteq\{1,\ldots,d\}$, and $\mathscr{C}_{\not s}$ denoting convolutions over the complementary dimensions $\not s$. When $\not s$ is empty, $\mathscr{C}_{\not s}$ is the identity and F_s reduces to the standard Fourier layer. The operator $\mathscr{R}$ transforms Fourier modes via $\mathscr{R}(\mathscr{F}_s\{\varepsilon\})_{\kappa,i}=\sum_{j=1}^{d_\varepsilon}R_{\kappa,i,j}\mathscr{F}_s\{\varepsilon\}_{\kappa,j}$, for $\kappa=0,1,\ldots,\kappa^{\max}$ and $i=1,\ldots,d_\varepsilon$, with learnable tensor $R\in\mathbb{C}^{\kappa^{\max}\times d_\varepsilon\times d_\varepsilon}$ and $\kappa^{\max}=\prod_{i\in s}\kappa_{(i)}^{\max}$.

3. Training Dataset

We consider two datasets of unstable flame development. The first is synthesized by solving 1D and 2D Sivashinsky equations modeling hybrid DL/DT instabilities, while the second is obtained from large-scale DNS.

3.1. Hybrid DL/DT Unstable Flame

The evolution of an unstable flame front in a d-dimensional periodic domain ($x\in\mathscr{D}=(0,2\pi]^d$) is modeled by the re-scaled Sivashinsky equation [9, 13]:

$$\frac{1}{\tau}\phi_t+\frac{1}{2\beta^2}(\nabla\phi)^2=-\frac{\mu}{\beta^4}\nabla^4\phi-\frac{\nu}{\beta^2}\nabla^2\phi+\frac{\rho}{\beta}\Gamma(\phi), \tag{4}$$

with $\Gamma(\phi)=\mathscr{F}^{-1}\{|\kappa|\,\mathscr{F}\{\phi\}\}$ (Fourier transforms over all dimensions) and parameters μ, ν, τ, β, ρ determined by the density ratio and Lewis number. Linearizing about $\phi=0$ yields the dispersion relation

$$\omega(\kappa)/\tau=-\mu(\kappa/\beta)^4+\nu(\kappa/\beta)^2+\rho(\kappa/\beta), \tag{5}$$

Following [13], a hybrid DL/DT instability is modeled by choosing $\rho\in[0,1]$ and $\beta>0$ with: (i) $\rho=1$ for pure DL (Michelson-Sivashinsky [14] with $\mu=0$, $\nu=-1$), (ii) $\rho=0$ for pure DT (Kuramoto-Sivashinsky [15] with $\mu=1$, $\nu=0$), (iii) $\nu=\mu-\rho$ (so that $\omega(\beta)=0$), (iv) $\omega_{\max}=\tau/4$, and (v) $\tau=\rho\beta/10+(1-\rho)$. This uniquely sets the parameters, with ρ blending instabilities and β controlling the maximum unstable wavenumber (see Figure 4).
For 1D, solutions are computed on a 256-point uniform grid for five cases with $\rho\in\{1,3/4,1/2,1/4,0\}$ at $\beta=25$. For each, 250 short-duration sequences ($0\le t\le 75$, 500 snapshots at $\Delta_t=0.15$) and one long-duration sequence ($0\le t\le 18\,750$, 125 000 snapshots) are generated; initial conditions $\phi(x,0)$ are sampled uniformly from $[0,0.03]$, with 10% held out for validation. For 2D, computations use a 128^2

Table 1: Relative L_2 training/validation errors for the FNO and kFNO models in all seven cases.

	(1D) β=25					(2D) β=15	DNS
	ρ=1	ρ=3/4	ρ=1/2	ρ=1/4	ρ=0	ρ=1/2	
FNO	0.020/0.020	0.011/0.011	0.010/0.010	0.0086/0.0093	0.011/0.012	0.0047/0.0048	non-converge
kFNO	0.0032/0.0035	0.0032/0.0035	0.0025/0.0025	0.0020/0.0022	0.0019/0.0019	0.0023/0.0023	0.0023/N.A.

grid; one hybrid case with $\rho = 1/2$ and $\beta = 15$ is considered (pure DL and DT cases at $\beta = 15$ are in [6]). Each case includes 45 sequences spanning $0 \le t \le 435.1$ with 5880 snapshots at $\Delta_t' = 0.074$, and initial conditions are low-wavenumber (spectral truncation for $|\kappa| > 8$), with a 1/9 validation split.

3.2. DNS Flame

Training data is extracted from a DNS of a DL-unstable premixed flame [10] that solves the reactive Navier-Stokes equations (assuming low Mach, one-step Arrhenius, unity Lewis) using high-order methods [16, 17, 18]. The simulation features an initially planar flame in a 2D periodic channel [10, 19, 20, 21, 22] for various channel widths Λ and density ratios. Here, we use a case with density ratio 8 and $\Lambda/l_f = 1536$ (with l_f the laminar flame thickness), which required roughly half million CPU hours. Defining $\beta' = \Lambda_c/\Lambda$ (with $\Lambda_c = 17\,l_f$), this DNS is comparable to setting $\beta = 90$ and $\rho = 1$ in Eq. (4) for a pure DL flame.

Flame fronts $\partial\Omega(t)$ are defined as the boundaries of $\Omega(t) = \{x \mid Y(x,t) > 0.6\}$ (with Y the fuel mass fraction) and are extracted via the marching squares method at $Y = 0.6$. The front is mapped to a 2D function

$$\Phi(x)|_{\partial\Omega} = \tanh(\gamma \cdot \varsigma/\Delta_*), \text{ with } \gamma = \inf_{\xi \in \partial\Omega \cap \{\xi_1 = x_1\}} |x_2 - \xi_2|, \quad \varsigma = \text{sign}(x \in \Omega), \tag{6}$$

and $\Delta_* = \Lambda/256$. The domain $\mathscr{D} = [0,\Lambda] \times [-0.45\Lambda, 1.15\Lambda]$ is discretized on a 256^2 grid. The DNS runs for $181\,\Lambda_c/s_f$ (with s_f the laminar flame speed), outputting 703 fronts at intervals of $\Delta_t'' = 0.26\,\Lambda_c/s_f$. Due to hardware limitations, n is set to 10 and the training data is paired in a 1-to-10 manner as $\{\Phi(x,t_j), [\Phi(x,t_{j+1}), \ldots, \Phi(x,t_{j+10})]\}_1^{693}$; no validation set is used.

4. Results and Discussions

For the synthesized Sivashinsky data, all kFNO models employ the standard Fourier layer with s covering all spatial dimensions. For the DNS flames, a modified Fourier layer is used where s corresponds only to the first dimension, so convolution is applied along the second dimension, therefore $\mathscr{C}_{\frac{1}{s}}$ is implemented by stacking two convolutional layers of stride 1, kernel size 3, padding 1 with replicate padding. This convolution better transforms $\Phi(x)$ with a persistent thin layer and steep gradient along x_2. Other implementation details follow [6]. Note that the baseline FNO is recovered from kFNO by setting $n = 1$ and merging $\bar{K}$ and $\bar{Q}$ into H, ensuring both models have equivalent expressive power and enabling a direct, unbiased comparison.

Table 1 summarizes the relative L_2 training/validation errors for 1D and 2D Sivashinsky flames, while Figure 2 shows the temporal evolution of the spatially averaged relative L_2 errors. Figure 1 presents random sequences of reference solution snapshots alongside predictions from kFNO and FNO for the 1D/2D cases and the DNS flame. Figure 3 compares the auto-correlation function

$$K(r) = \mathbb{E}(g(r)/g(0)), \quad g(r) = \int_{\mathscr{D}} \phi(x,t^*)\,\phi(x-r,t^*)\,dx, \tag{7}$$

with t^* sufficiently late, computed from both the reference and predicted solutions. Figure 4 compares the 1D reference dispersion relation (Eq. (5)) with those obtained from kFNO and FNO via the operator

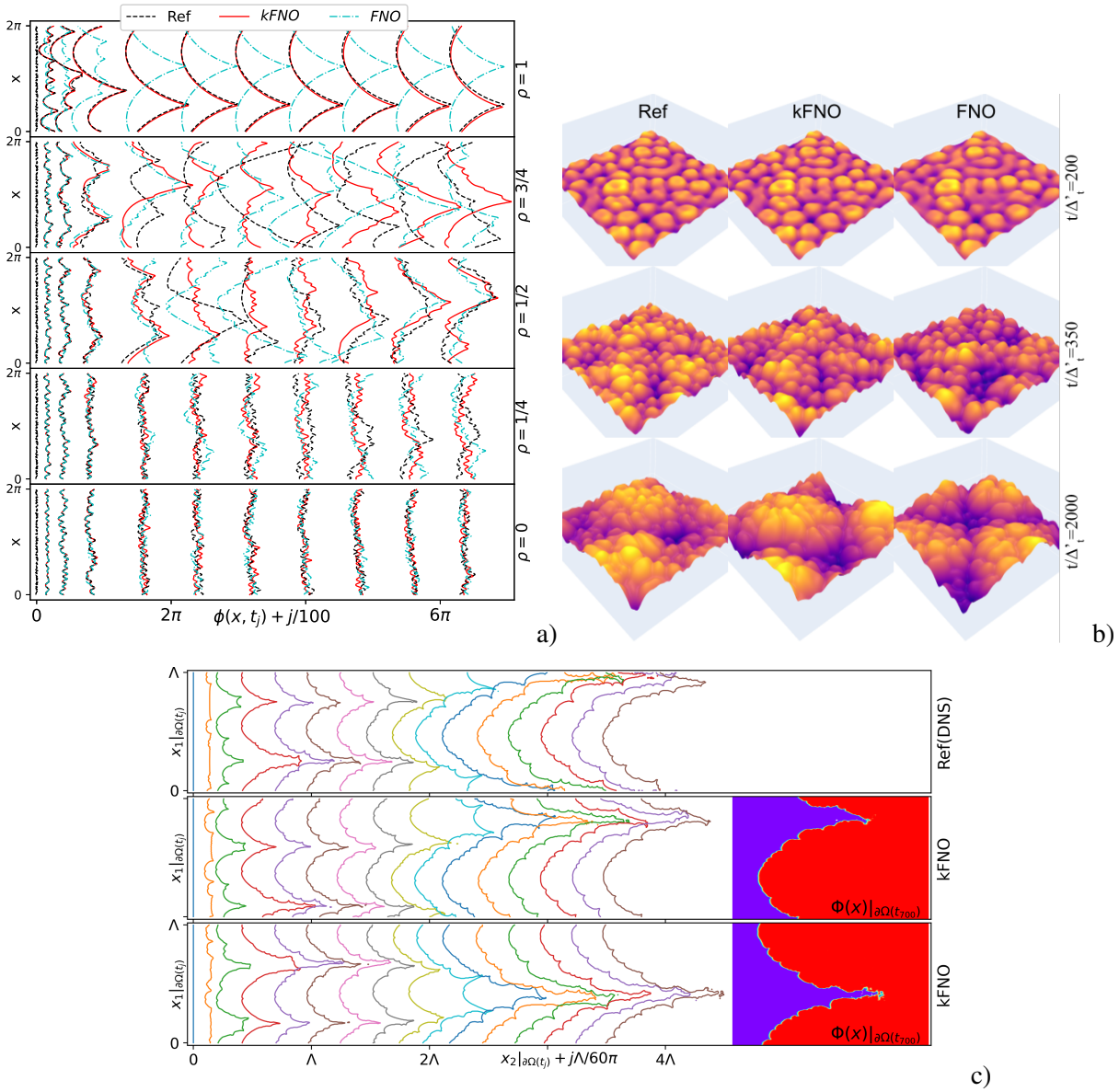

Figure 1: Comparison of random sequences of reference flame solutions with predictions from kFNO and FNO. (a) 1D Sivashinsky flames $\phi(x,t_j)$ for five cases with $\beta = 25$, plotted at indices $j \in \{0, 50, 125\} \cup \{250k : k = 1, \ldots, 8\}$. (b) A 2D Sivashinsky flame at $\rho = 1/2$ and $\beta = 15$. (c) DNS flame fronts $\partial\Omega(x,t_j)$ compared with two random sequences of predicted fronts by kFNO (FNO fails to converge) at indices $j \in \{0, 25\} \cup \{50k : k = 1, \ldots, 14\}$; the inset shows $\Phi(x,t_j)$ at $j = 700$, Eq. (6).

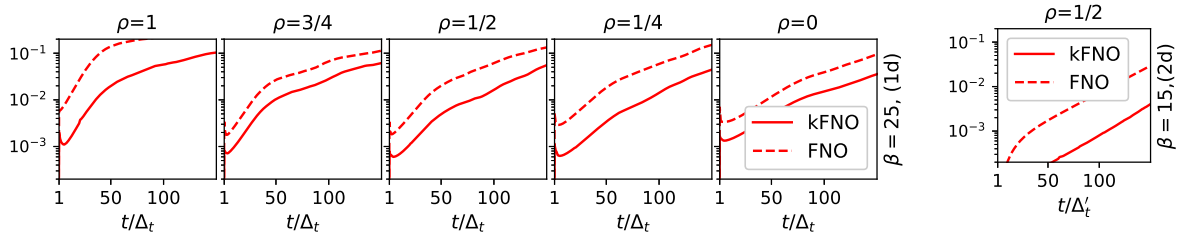

Figure 2: Temporal evolution of the relative L_2 error, averaged over space and 10 random solution instances, for kFNO and FNO applied to learning the 1D and 2D Sivashinsky flames.

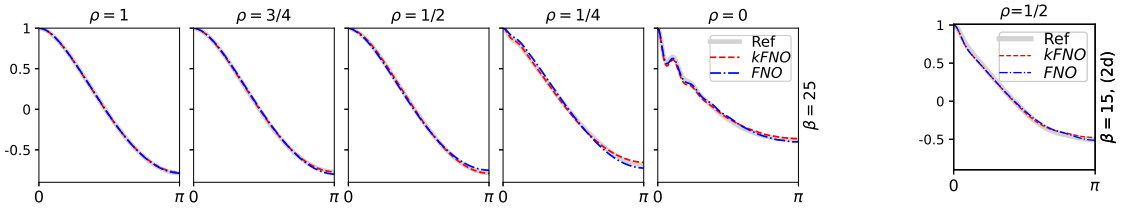

Figure 3: Comparison of the auto-correlation functions(Eq. 7) computed from long-term reference solutions with those predicted by kFNO and FNO for the 1D and 2D Sivashinsky equations.

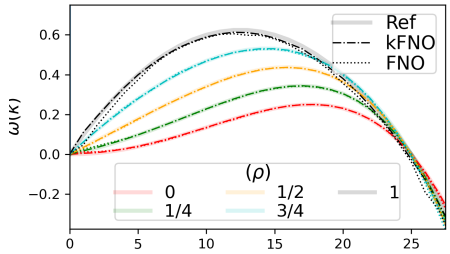

Figure 4: Comparison of the reference dispersion relations, Eq. (5), for five 1D Sivashinsky flame cases at $\beta = 25$, with those computed for kFNO and FNO based on the operator Jacobian, Eq. (8) .

Jacobian, approximated as

$$\omega(\kappa) \approx \frac{\log(J(\kappa,\kappa))}{n\Delta_t}, \quad J(\kappa,\kappa') = \frac{\partial}{\partial a_\kappa}\left|\mathscr{F}\left\{\bar{\mathscr{G}}_n\left(2a_\kappa\cos(\kappa x)\right)\right\}_{\kappa'}\right|, \tag{8}$$

computed using automatic differentiation (e.g., PyTorch.autograd.functional.jacobian).
Key observations include:

- kFNO yields more accurate short-term predictions than FNO in all hybrid DL/DT cases for both 1D and 2D flames, with training/validation errors 2–6 times lower (see Table 1 and Figure 2). Figure 4 shows that kFNO produces slightly more accurate dispersion relations.
- Both models capture long-term statistics, as evidenced by the auto-correlation functions in Figure 3.
- A 2D kFNO variant with a convolutional Fourier layer (Eq. 3) successfully learns complex DNS flame fronts (Figure 1) while FNO fails to converge (Table 1).
- kFNO is more computationally efficient, requiring about 60% of the training time of FNO and exhibiting a faster decrease in training error over epochs.

5. Summary and Conclusion

This study explores the application of the Koopman-inspired Fourier Neural Operator (kFNO) to modeling flame front instabilities, specifically hybrid Darrieus-Landau (DL) and Diffusive-Thermal (DT) instabilities, as well as complex fractal-like flame structures from direct numerical simulations (DNS). By leveraging a high-dimensional latent space, kFNO improves both short-term accuracy and long-term statistical fidelity, addressing challenges in operator learning for chaotic systems.
Results demonstrate that kFNO effectively captures the nonlinear dynamics of unstable flames while maintaining stability in long-horizon predictions. The method outperforms conventional Fourier Neural Operators (FNO) in preserving physical characteristics and reducing error accumulation. These findings highlight kFNO's potential for advancing data-driven modeling of combustion instabilities and other complex PDE-governed phenomena.

Acknowledgments

The authors gratefully acknowledge the financial support by the Swedish Research Council (VR-2019-05648). The computations were enabled by resources provided by the National Academic Infrastructure for Supercomputing in Sweden (NAISS), at ALVIS and Tetralith, partially funded by the Swedish Research Council through grant agreement no. 2022-06725.

References

[1] L. Lu, P. Jin, and G.E. Karniadakis. Deeponet: Learning nonlinear operators for identifying differential equations based on the universal approximation theorem of operators. 2019.

[2] Z. Li, N. Kovachki, K. Azizzadenesheli, B. Liu, K. Bhattacharya, A. Stuart, and A. Anandkumar. Fourier neural operator for parametric partial differential equations. 2020.

[3] B.O. Koopman. Hamiltonian systems and transformation in hilbert space. *Proceedings of the National Academy of Sciences*, 17(5):315–318, 1931.

[4] S.L. Brunton and J.N. Kutz. *Data-driven science and engineering: Machine learning, dynamical systems, and control*. Cambridge University Press, 2022.

[5] I. Mezić. Analysis of fluid flows via spectral properties of the koopman operator. *Annual review of fluid mechanics*, 45(1):357–378, 2013.

[6] R. Yu, M. Herbert, M. Klein, and E. Hodzic. Koopman theory-inspired method for learning time advancement operators in unstable flame front evolution. *Physics of Fluids*, 37:024115, 2025.

[7] G. Darrieus. Propagation d'un front de flamme. *Unpublished work presented at La Technique Moderne*, 1938.

[8] YB Zeldovich. Theory of combustion and detonation of gases. In *Selected Works of Yakov Borisovich Zeldovich, Volume I: Chemical Physics and Hydrodynamics*. Princeton University Press, 1944.

[9] G.I.Sivashinsky. Nonlinear analysis of hydrodynamic instability in laminar flames—i. derivation of basic equations. *Acta Astronautica*, 4:1177–1206, 1977.

[10] R. Yu, X.S. Bai, and V. Bychkov. Fractal flame structure due to the hydrodynamic darrieus-landau instability. *Phys. Rev. E*, 92(6):063028, 2015.

[11] R. Yu. Deep learning of nonlinear flame fronts development due to darrieus–landau instability. *APL Machine Learning*, 1(2):026106, 2023.

[12] R. Yu and E. Hodzic. Parametric learning of time-advancement operators for unstable flame evolution. *Physics of Fluids*, 36:044109, 2024.

[13] R. Yu, E. Hodzic, and KJ Nogenmyr. Learning flame evolution operator under hybrid darrieus landau and diffusive thermal instability. *Energies*, 17(13):3097, 2024.

[14] Daniel M Michelson and Gregory I Sivashinsky. Nonlinear analysis of hydrodynamic instability in laminar flames—ii. numerical experiments. *Acta astronautica*, 4(11-12):1207–1221, 1977.

[15] Yoshiki Kuramoto. Diffusion-induced chaos in reaction systems. *Progress of Theoretical Physics Supplement*, 64:346–367, 1978.

[16] R. Yu, J.F. Yu, and X.S. Bai. An improved high-order scheme for DNS of low Mach number turbulent reacting flows based on stiff chemistry solver. *J. Comput. Phys.*, 231(16):5504, 2012.

[17] R. Yu and X.S. Bai. A fully divergence-free method for generation of inhomogeneous and anisotropic turbulence with large spatial variation. *J. Comput. Phys.*, 256:234, 2014.

[18] R. Yu and X.S. Bai. A semi-implicit scheme for large Eddy simulation of piston engine flow and combustion. *Int. J. Numer. Methods Fluids*, 71(1):13, 2013.

[19] J.F. Yu, R. Yu, X.S. Bai, M.B. Sun, and J.G. Tan. Nonlinear evolution of 2d cellular lean hydrogen/air premixed flames with varying initial perturbations in the elevated pressure environment. *International Journal of Hydrogen Energy*, 42(6):3790–3803, 2017.

[20] R. Yu and A.N. Lipatnikov. Surface-averaged quantities in turbulent reacting flows and relevant evolution equations. *Phys. Rev. E*, 100:013107, 2019.

[21] R. Yu, T. Nillson, X.S. Bai, and A.N. Lipatnikov. Evolution of averaged local premixed flame thickness in a turbulent flow. *Combust. Flame*, 207:232–249, 2019.

[22] R. Yu, T. Nilsson, C. Fureby, and A.N. Lipatnikov. Evolution equations for the decomposed components of displacement speed in a reactive scalar field. *Journal of Fluid Mechanics*, 911, 2021.